

Magnetic Reconnection Characteristics and Their Influence on the Reconnection Rate in the Earth's Magnetotail

Nurumira Ashikin^a, Wai-Leong Teh^{a*} & Mardina Abdullah^{a,b}

^aSpace Science Centre, Institute of Climate Change, Universiti Kebangsaan Malaysia, Malaysia

^bDepartment of Electrical, Electronic and System Engineering,

Faculty of Engineering & Built Environment, Universiti Kebangsaan Malaysia, Malaysia

*Corresponding author: wteh@ukm.edu.my

Received 12 February 2025, Received in revised form 22 June 2025
 Accepted 22 July 2025, Available online 30 October 2025

ABSTRACT

Magnetic reconnection is an essential mechanism in the collisionless plasmas that enables the transformation of magnetic energy into plasma kinetic energy and thermal energy. The efficiency of energy conversion during magnetic reconnection is measured by the rate of reconnection. This article focuses on investigating the relationships between reconnection characteristics and the reconnection rate, via in-situ observations (including measurements of magnetic field, electric field, ion and electron plasma moments) of magnetic reconnection in the Earth's magnetotail, as recorded by the Cluster spacecrafts from 2001 to 2005. Thirteen reconnection x-line events were selected for examining correlation coefficients (r) between the reconnection rate and reconnection characteristics (e.g., current sheet thickness, current density, lobe magnetic field, inflow speed, Alfvén speed, reconnection electric field, and converging electric field). The correlations of the reconnection characteristics were classified into three categories, i.e., $|r| > 0.6$ (good), $0.3 < |r| \leq 0.6$ (ambiguous), and $0 < |r| \leq 0.3$ (no correlation). The results show that a good correlation is obtained for lobe magnetic field, inflow speed, and converging electric field, while an ambiguous correlation is observed for reconnection electric field and current density. No correlation is found for Alfvén speed and current sheet thickness. This study provides insights into key physical parameters that influence fast magnetic reconnection (lobe magnetic field, inflow speed and converging electric field) and highlights the complexity of reconnection processes that may cause unresolved correlation in space plasma dynamics.

Keywords: Magnetic reconnection; reconnection rate; magnetotail; current sheet; collisionless plasmas

INTRODUCTION

Magnetic reconnection is referred to as the key process for energy conversion wherein the magnetic energy is transformed into directed particle kinetic and thermal energy by altering the configuration of the magnetic field. This process explains numerous dynamics of plasma phenomena, ranging from microscopic to macroscopic scale. It holds a vital part in the plasma transportation between two different regimes in space, particle acceleration and radiation (Hesse et al. 2020). Reconnection signatures are also observed in various phenomena, notably in solar activities, stellar flares, plasma laboratories, and other

astrophysical settings, proving their universal significance in plasma physics. Magnetic reconnection initially takes place at a null point (x-line) in a tiny diffusion region characterized by two distinct scales, namely the ion and electron inertial lengths before extending its effect to global regime. In the diffusion region, the electrons remain magnetized and coupled to the magnetic field (Pontin et al. 2024). In contrast to electrons, ions are demagnetized which would lead to charge separation, bipolar electric field and quadrupole magnetic field (Cheng et al. 2021). The plasmas different motions lead to the Hall effect, which will then induce the reconnection electric field at the reconnection site, hence controlling the rate of reconnection (Li et al. 2021).

The rate of reconnection, which measures the change of magnetic flux involved in the reconnection process, indicates the efficiency of energy conversion during magnetic reconnection. It can be quantified across multiple approaches (Ni et al. 2020). Essentially, it is measured as the average inflow speed (v_{in}) ratio to the outflow speed (v_{out}). During magnetic reconnection, the outflow speed is accelerated to the Alfvén speed, where B and ρ are the magnetic field strength and the plasma density in the inflow region. In practice, the reconnection electric field, normalized by the product of B and v_{alf} , is applied to estimate the reconnection rate (e.g., Liu et al. 2025; Macek et al. 2019). Previous reconnection studies showed that the normalized fast reconnection rate was estimated around 0.1 in kinetic regimes (Liu et al. 2022). How the fast reconnection is generated, or which reconnection characteristics facilitate the fast reconnection rate is an outstanding issue in reconnection physics (Pucci et al. 2020). Using the magnetotail observations by the Geotail spacecraft, Imada et al. (2011) examined the correlation between energetic electron acceleration efficiency with several reconnection characteristics (e.g., ion and electron temperatures, Hall electric field, reconnection rate, and satellite location). They concluded that the energetic electron acceleration efficiency was highly correlated with the ion and electron heating but was ambiguously correlated with the reconnection rate.

In this study, the relationships of the reconnection characteristics with the reconnection rate are investigated, using in-situ magnetotail reconnection observations by ESA's Cluster spacecraft from 2001–2005. The reconnection characteristics studied are current sheet thickness, current density, reconnection electric field, lobe magnetic field, inflow speed, Alfvén speed, and converging electric field. The methodology used by Imada et al. (2011) is adopted to calculate the current sheet thickness, lobe magnetic field, and inflow speed. Thirteen reconnection x-line events were selected for the analysis. This paper will further refine the foundational understanding of reconnection physics, especially in identifying the roles and relative contributions of various plasma properties in controlling the dynamics and efficiency of magnetic reconnection as recognizing which properties are affecting the rate is important to ultimately understand other related mechanisms such as energetic electron dynamics and the energy conversion process during magnetic reconnection.

METHODOLOGY

We obtained the relevant data from the Cluster spacecraft, which comprised a constellation of four similar units,

designated as C1, C2, C3, and C4, arranged in a tetrahedral formation in space. Identical sets of scientific payloads were carried by the four spacecraft. The magnetic field data utilized in this investigation had been collected using the fluxgate magnetometer (FGM) (Balogh et al. 2001). The measurements of the electric field data were conducted through the Electric Field and Wave experiment (EFW) (Gustafsson et al. 2001). The ion plasma moments were provided by the Cluster Ion Spectrometry Hot Ion Analyzer (CIS/HIA) (Rème et al. 2001). Additionally, the energetic electron spectrogram and flux were analyzed by the Research with Adaptive Particle Imaging Detectors (RAPID) (Wilken et al. 2001), and the electron plasma moments were supplied by the Plasma Electron and Current Experiment (PEACE) (Johnstone et al. 1997). Note that the HIA data were limited to C1 and C3 only and that the electric field data were only measured by four wire poles in the spin plane of the spacecraft (\sim x-y Geocentric Solar Ecliptic (GSE)), while the out-of-plane component was estimated by the assumption. In this study, unless otherwise noted, we used a consistent sampling rate of 4 s for all the instrument data. The vector components were shown in the GSE coordinates system throughout the paper. For a nominal, two-dimensional magnetotail reconnection, the high-speed reconnection outflow is directed along the GSE-x axis, with the GSE-z axis serving as the normal direction to the current sheet, and the GSE-y axis being the direction perpendicular to the reconnection plane (i.e., the x-z plane).

Eastwood et al. (2010) surveyed 175 magnetotail passes and subsequently identified 33 reconnection x-line events in the magnetotail during 2001 – 2005, for which the reversals of the high-speed reconnection outflow and the normal component of the magnetic field were correlated. The presence of a reconnection x-line suggested that the reconnection diffusion region was observed. Numerous previous papers have used these events for multiple purposes. In this study, only 13 out of 33 reconnection x-line events were investigated because, for some events, the PEACE data were contaminated by the byte-swap data corruption (Teh et al. 2012). Table 1 summarizes the mathematical formulations for computing the reconnection rate and the reconnection characteristics studied here, where n is the ion plasma density and ρ is the mass density. Note that the E_y is used as the reconnection electric field (E_r), and the E_z is the converging electric field normal to the current sheet. Finally, MATLAB was extensively used to calculate and analyze of the observational data.

TABLE 1. Formulae for estimating the reconnection rate and the reconnection characteristics

Abbreviation	Parameter	Formula (units)
j	current density	$qn(v_i - v_e)^*$ (nA/m ²)
B_{lobe}	lobe magnetic field	$\sqrt{B^2 + 2\mu_0 nk_b(T_i + T_e)}$ (nT)
HCS	half current sheet thickness	$B_{\text{lobe}}/(\mu_0 j_y)$ (km)
v_{inf}	plasma inflow speed	E_y/B_{lobe} (km/s)
v_{alf}	Alfvén speed	$B/\sqrt{\mu_0 \rho}$ (km/s)
rate	reconnection rate	$E_y \sqrt{\mu_0 \rho}/B_{\text{lobe}}^2$

* q is the magnitude of the elementary charge

RESULTS AND DISCUSSION

Figure 1 illustrates the general summary of a reconnection x-line event that appeared around $(-18.92, -1.94, -0.89) R_E$ (the Earth's radius) in the Earth magnetotail on 27 August 2001 between 04:03 UT – 04:09 UT. The color codes for each spacecraft are C1: black, C2: red, C3: green and C4: blue. From the upper panel to the lower panel, the figure displays (a) the magnetic field strength, (b) - (d) the three magnetic field components, and (e) - (g) the three ion velocity components. The high-speed reconnection outflow, which depends on the magnetic energy released, is considered as one of the indicators of magnetic reconnection. Here, it was seen ($|v_x| > 300$ km/s), and its sign was gradually reversed from negative to positive as shown in Figure 1(e). The B_z reversal was also detected, as indicated by the black dashed line in Figure 1(d), about 10 s after the v_x reversal. It is suggested that the reconnection x-line moved tailward relative to the spacecraft's location, which aligned with the orientation of the pressure gradient (Leonenko et al. 2021). At $\sim 04:03:52$ UT, as highlighted by the red dashed line, C1 crossed the current sheet shortly ($B_x = 0$) but stayed in the northern lobe ($B_x > 0$) afterward.

Figure 2 shows (a) the ion density for C1 (black) and C3 (green); (b) - (d) the electron energy-time spectrograms for pitch angles 0° , 180° , and 90° , and (e) the energetic electron flux between 04:03 UT – 04:09 UT. It was found that the electrons mostly moved in the directions parallel (0°) and anti-parallel (180°) to the magnetic fields consistent with reconnection-driven dynamics. No significant increase in the energetic electron flux was detected during this particular event. As shown in Figure 3(c), the bipolar electric fields move at a different scale in the diffusion region, were detected and aligned with the direction where reconnection is the most intense. Overall, the observed fluctuations in the electric field and current density near the red and black dashed lines suggest the movement of the C1 spacecraft across different areas of the reconnection site, reflecting variations in plasma dynamics and electric field topology.

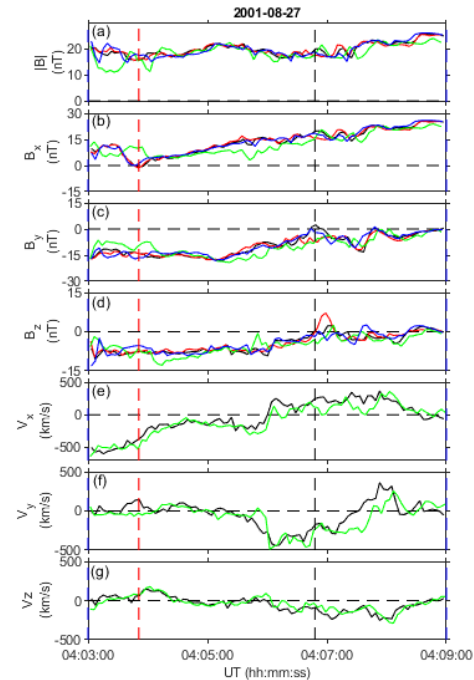


FIGURE 1. Overview of a reconnection x-line event observed by the Cluster spacecrafts in the magnetotail on 27 August 2001 between 0403 UT – 0409 UT. The panels show (a) – (d) the magnetic fields and (e) – (g) the ion plasma velocities. The red dashed line denotes the current sheet crossing by C1 and the black dashed line marks the B_z reversal.

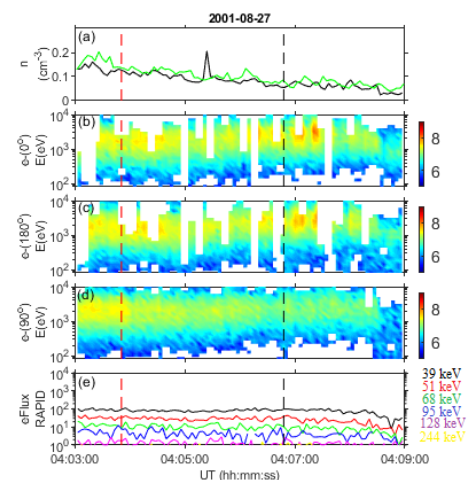
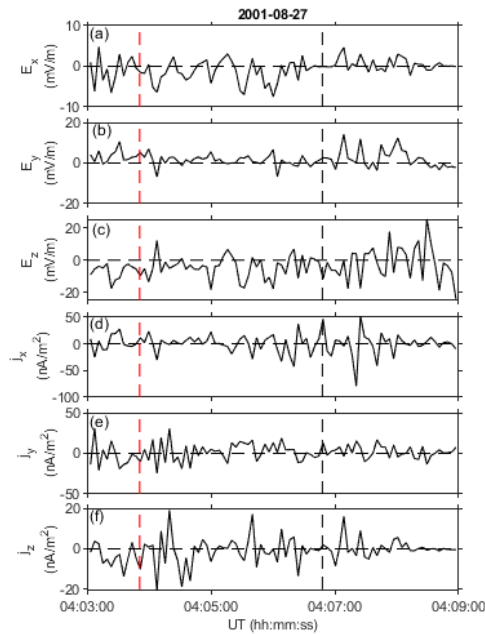


FIGURE 2. Measurements of (a) the ion density, (b) - (d) the electron energy-time spectrogram for three pitch angles (parallel (0°), anti-parallel (180°), and perpendicular (90°)) and (e) the energetic electron flux, between 0403 UT – 0409 UT.

TABLE 2. Overview of the analytical findings for the reconnection characteristics for 13 events.

Date	Time interval (UT)	Mean value of magnetic reconnection characteristics								Mean rate
		$B_{\text{Lobe}} \times 10^{-9}$ (T)	HCS $\times 10^{-3}$ (km)	$j_x \times 10^{-9}$ ($\frac{\text{A}}{\text{m}^2}$)	$j_y \times 10^{-9}$ ($\frac{\text{A}}{\text{m}^2}$)	v_{inf} ($\frac{\text{km}}{\text{s}}$)	V_{alf} ($\frac{\text{km}}{\text{s}}$)	$E_r \times 10^{-3}$ ($\frac{\text{V}}{\text{m}}$)	$E_z \times 10^{-3}$ ($\frac{\text{V}}{\text{m}}$)	
27/08/2001	0403-0409	19.81	1.22	17.72	1.26	99.98	567.14	1.89	-3.81	0.08
18/08/2002	1707-1709	12.25	3.65	19.33	10.98	-12.66	1120.68	-0.23	1.36	0.02
21/08/2002	0815-0819	11.03	15.67	18.59	0.24	476.24	1690.56	4.75	-0.73	0.35
18/09/2002	1309-1315	23.02	2.33	14.66	1.19	133.61	1749.48	3.10	-2.08	0.08
02/10/2002	2120-2121	7.05	0.33	16.38	7.45	455.16	820.04	3.94	-6.38	0.48
26/10/2002	0918-0923	31.76	8.36	16.07	-1.22	156.27	3302.61	5.26	-0.95	0.04
01/09/2003	0431-0435	13.18	0.99	22.38	5.90	78.78	559.48	1.05	-0.53	0.16
19/09/2003	2329-2331	13.69	1.12	24.99	9.83	192.02	1464.57	2.68	-4.78	0.16
04/10/2003	061830-062145	19.45	0.34	23.86	1.57	-29.62	1730.82	-0.76	4.72	0.00
09/10/2003	0223-0227	10.72	0.44	29.05	2.54	415.40	1125.29	4.38	1.04	0.48
14/09/2004	230445-2306	9.27	0.20	32.04	20.17	409.12	1099.65	3.43	-18.67	0.58
03/10/2004	1814-1817	25.86	2.35	17.83	1.54	89.80	1581.03	2.51	0.08	0.05
26/09/2005	0943-0951	19.39	0.39	23.02	12.13	24.16	567.14	0.65	0.09	0.03

FIGURE 3. (a) – (c) the three electric field components (E_x , E_y , E_z) and (d) – (f) the three current density components (j_x , j_y , j_z) between 0403 UT – 0409 UT.

Results of the lobe magnetic field, half current sheet thickness (HCS), inflow speed, Alfvén speed, and the reconnection rate are displayed in Figure 4, based on C1 spacecraft. Two HCS values were calculated at the two dashed lines (the blue and red diamonds); the blue diamond is when C1 was in the current sheet and the red diamond was during the x-line crossing. The HCS was found to be smaller near the x-line due to the low pressure caused by

the decreasing plasma density. This low pressure localized the current density to a narrow scale through the ion-electron decoupling hence also explaining the increased average value of current density around this time (Pucci et al. 2020). Moreover, the inflow speed and the reconnection rate increased shortly after C1 crossed the x-line around 04:07:08 UT (see Figures 4(c) and 4(e)). This outcome aligns with prior studies by Genestreti et al. (2018)

and Macek et al. (2019) where the inflow speed and the reconnection rate increased when passing through the reconnection onset around this time indicating that the total magnetic flux transfer between the plasma inflow and the outflow region where the flux are being carried away. The lobe magnetic field exhibited relative stability but showed a slight increase around 04:06:55 UT prior to the increase in the reconnection rate, suggesting that it may facilitate a more efficient reconnection event by supplying the magnetic energy that is transformed into plasma energy. In addition, the Alfvén speed in Figure 4(d) increases, likely due to the increasing lobe magnetic field, which will affect the normalization of the reconnection rate. However, the rate itself is more strongly influenced by the inflow speed relative to the Alfvén speed rather than by its absolute value. Other than that, Hall field also becomes stronger during the narrowing of the current sheet.

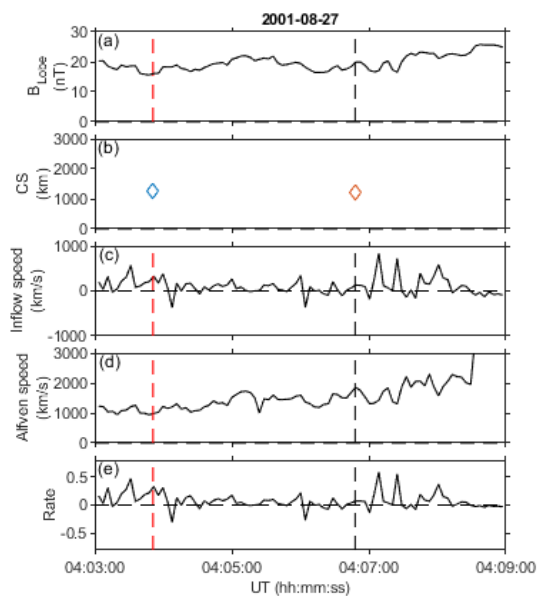


FIGURE 4. Analysis results of (a) B_{lobe} , (b) HCS, (c) v_{inP} , (d) v_{alf} and (e) rate for the 27 August 2001 event.

The analysis results of the thirteen events were summarized in Table 2. 10 out of the 13 events were tailward reconnection, which aligns with the findings by Ieda & Miyashita (2024) who reported that most of the x-lines move tailward. It was revealed that for most events, the magnetic field lobe decreased as the E_y and E_z increased during the reconnection process. The counterstreaming field-aligned electrons were present for

all of the events consistent with previous findings. Additionally, it is well established that thinner current sheets also exhibit a higher energetic electron flux (for which the results were not shown in this paper).

Next, we analyzed which factors may be responsible for a fast reconnection. Figure 5 shows the relationships of the eight reconnection characteristics with the reconnection rate, where the magenta line is the regression line and the correlation coefficient (r) is calculated to determine which of the reconnection characteristics contributed to fast reconnection rate. Using the classification system by Imada et al. (2011), the r values were classified into three categories, namely $|r| > 0.6$ (good correlation), $0.3 < |r| \leq 0.6$ (ambiguous correlation), and $0 < |r| \leq 0.3$ (no correlation). The lobe magnetic field, inflow speed, and converging electric field correlate well with the reconnection rate, while an ambiguous correlation is obtained for the current density and the reconnection electric field. No correlation is found for the Alfvén speed and half current sheet.

A good correlation is expected for the lobe magnetic field and inflow speed, as both parameters directly contribute to the calculation of the reconnection rate (see Table 1). This relationship occurs because the inflow speed regulates the mass and energy flux entering the reconnection region, whereas the intensity of the lobe magnetic field determines the magnetic energy available for conversion during the process. The unexpected result is that the E_r is not highly correlated ($r \approx 0.58$) with the reconnection rate since the E_r is part of the rate calculation (see Table 1). The reason for this unexpected result is unclear yet despite the E_r value being approximately 1 - 10 mV/m, which falls within the range of a fast reconnection (Wang et al. 2023). However, a possible explanation for this result may be due to the temporal cause or other dynamic processes that may not be fully captured in the analyzed dataset. The electric field values used in this analysis are averaged over a certain time interval. Despite using the identical time frame for reconnection rate, the electric field data may not precisely reflect the conditions at the x-line crossing during reconnection, potentially causing a difference in the analysis. Besides that, recent review also suggests that the degree of plasma ionization may affect the reconnection process (Ni et al. 2020). While this unpredictability is a recognized characteristic of reconnection, it does not undermine the reliability of the data; instead, it highlights the challenge of directly correlating these parameters.

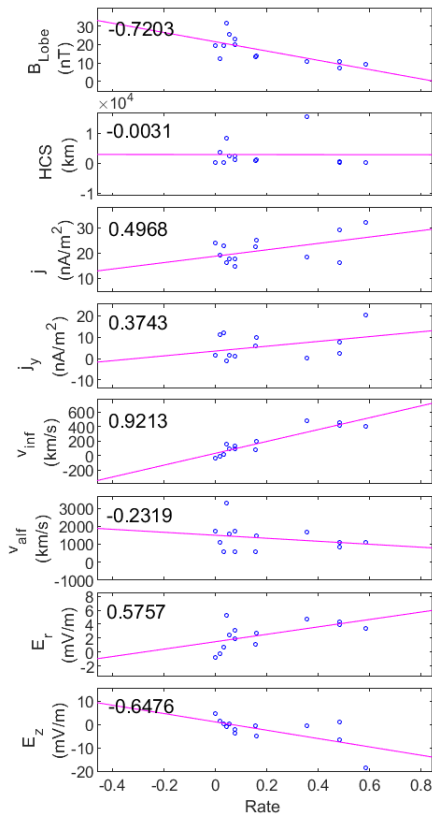


FIGURE 5. Correlation results for the reconnection characteristics (magnetic field lobe, half current sheet thickness, current density, y-component of current density, inflow speed, Alfvén speed, reconnection electric field, converging electric field) for 13 events.

In theory, the current sheet thickness should exhibit an inverse correlation with the reconnection rate as thinner current sheets are expected to enhance the reconnection process by causing stronger magnetic field and higher current densities. It has long been argued that the formation of thin current sheet, either by two-fluid scale or plasmoid (magnetic island or flux rope) instability, is necessary for fast reconnection. The basis for the finding in this study is not entirely clear, indicating that further investigation is required to thoroughly grasp the underlying reconnection mechanisms. Meanwhile, a good correlation for the converging electric field aligns with the findings of Imada et al. (2011). Moreover, the previous findings indicated that the reconnection rate was initially governed by the converging electric field. This finding aligns with the theoretical framework where the converging electric field facilitates the plasma inflow towards the magnetic reconnection region, thus maintaining the reconnection rate and contributes to determining the overall efficiency of magnetic flux conversion.

Some of the unexpected outcomes may stem from time-varying factors or other dynamic processes that are not entirely accounted for. The variability in the reconnection region may cause fluctuations that are not captured within the selected observation intervals. Additionally, plasma processes such as turbulence or wave-particle interactions due to the particle distribution, may affect the measured parameters, leading to deviations from the expected correlations. However, future work involving higher temporal resolution or advanced cross-correlation analysis techniques with more extensive data could provide deeper insights and help better understand these dynamic relationships.

CONCLUSION

This paper aimed to investigate the correlation between various reconnection characteristics (e.g., lobe magnetic field, current sheet thickness, inflow speed, Alfvén speed, reconnection electric field, converging electric field, and current density) and the reconnection rate by studying thirteen magnetotail reconnection x-line events observed by Cluster spacecraft from 2001 to 2005. The results show that a good correlation was obtained for the lobe magnetic field, inflow speed, and converging electric field. Interestingly, the ambiguous correlation observed for the reconnection electric field and current density deviates from theory, which predict a good correlation (albeit inversely for current density) between the two parameters and the reconnection rate. Furthermore, no correlation was found between Alfvén speed and current sheet thickness, despite previous study suggesting an inverse correlation with the latter. These results suggest that lobe magnetic field, inflow speed and converging electric field would be the favorable conditions for a fast reconnection rate. However, the weak correlation for the reconnection electric field raises questions about the temporal and dynamics involved in these events, while the absence of a clear relationship for current sheet thickness presents an opportunity for further investigation to explore the mechanisms causing these differences. The findings of this study open up potential direction for future studies, mainly exploring the characteristics that have a favorable correlation with the reconnection rate including asymmetric reconnection in magnetopause where the plasma densities are vastly different between both sides. Besides that, the unexpected discrepancies also can be relevant and contribute to a deeper understanding of their roles in facilitating fast reconnection events.

ACKNOWLEDGEMENT

This study was funded by a grant from Universiti Kebangsaan Malaysia (GP-K020730). We express our gratitude to ESA for the freely available Cluster data.

DECLARATION OF COMPETING INTEREST

None.

REFERENCES

- Balogh, A., Carr, C. M., Acuña, M. H., Dunlop, M. W., Beek, T. J., Brown, P., Fornacon, K. H., Georgescu, E., Glassmeier, K. H., Harris, J., Musmann, G., Oddy, T. & Schwingenschuh, K. 2001. The cluster magnetic field investigation: Overview of in-flight performance and initial results. *Ann. Geophys* 19(10/12): 1207-1217.
- Cheng, C. Z., Inoue, S., Ono, Y., Tanabe, H., Horiuchi, R. & Usami, S. 2021. Plasma heating and current sheet structure in anti-parallel magnetic reconnection. *Physics of Plasmas* 28(7): 072101.
- Eastwood, J. P., Phan, T. D., Øieroset, M. & Shay, M. A. 2010. Average Properties of the magnetic reconnection ion diffusion region in the earth's magnetotail: The 2001–2005 cluster observations and comparison with simulations. *Journal of Geophysical Research: Space Physics* 115(A8):
- Genestreti, K. J., Nakamura, T. K. M., Nakamura, R., Denton, R. E., Torbert, R. B., Burch, J. L., Plaschke, F., Fuselier, S. A., Ergun, R. E., Giles, B. L. & Russell, C. T. 2018. How accurately can we measure the reconnection rate v_m for the mms diffusion region event of 11 July 2017. *Journal of Geophysical Research: Space Physics* 123(11): 9130-9149.
- Gustafsson, G., André, M., Carozzi, T., Eriksson, A. I., Fälthammar, C.-G., Grard, R., Holmgren, G., Holtet, J., Ivchenko, N. & Karlsson, T. 2001. First results of electric field and density observations by cluster EFW based on initial months of operation. *Annales Geophysicae*, hlm. 1219-1240.
- Hesse, M. & Cassak, P. A. 2020. Magnetic reconnection in the space sciences: Past, present, and future. *Journal of Geophysical Research: Space Physics* 125(2): e2018JA025935.
- Ieda, A. & Miyashita, Y. 2024. Duskward displacement of plasmoids and reconnection in the near-earth magnetotail. *Earth, Planets and Space* 76(1): 159.
- Imada, S., Hirai, M., Hoshino, M. & Mukai, T. 2011. Favorable conditions for energetic electron acceleration during magnetic reconnection in the earth's magnetotail. *J. Geophys. Res.* 116(A08217):
- Johnstone, A. D., Alsop, C., Burge, S., Carter, P. J., Coates, A. J., Coker, A. J., Fazakerley, A. N., Grande, M., Gowen, R. A., Gurgiolo, C., Hancock, B. K., Narheim, B., Preece, A., Sheather, P. H., Winningham, J. D. & Woodliffe, R. D. 1997. Peace: A plasma electron and current experiment. Dlm. *The Cluster and Phoenix Missions*, disunting oleh Escoubet, C. P., Russell, C. T. & Schmidt, R., 351-398. Dordrecht: Springer Netherlands.
- Li, T., Priest, E. & Guo, R. 2021. Three-dimensional magnetic reconnection in astrophysical plasmas. *Proceedings of the Royal Society A.* 477(2249): 20200949.
- Liu, Y.-H., Cassak, P., Li, X., Hesse, M., Lin, S.-C. & Genestreti, K. 2022. First-principles theory of the rate of magnetic reconnection in magnetospheric and solar plasmas. *Communications Physics* 5(1): 97
- Liu, Y.-H., Hesse, M., Genestreti, K., Nakamura, R., Burch, J. L., Cassak, P. A., Bessho, N., Eastwood, J. P., Phan, T. & Swisdak, M. 2025. Ohm's Law, the reconnection rate, and energy conversion in collisionless magnetic reconnection. *Space Science Reviews* 221(1): 16.
- Leonenko, M. V., Grigorenko, E. E. & Zelenyi, L. M. 2021. Spatial scales of super thin current sheets with MMS observations in the earth's magnetotail. *Geomagnetism and Aeronomy* 61(5): 688-695.
- Macek, W. M., Silveira, M. V. D., Sibeck, D. G., Giles, B. L. & Burch, J. L. 2019. Mechanism of reconnection on kinetic scales based on magnetospheric multiscale mission observations. *The Astrophysical Journal* 885(1): L26.
- Nakamura, T. K. M., Genestreti, K. J., Liu, Y.-H., Nakamura, R., Teh, W.-L., Hasegawa, H., Daughton, W., Hesse, M., Torbert, R. B., Burch, J. L. & Giles, B. L. 2018. Measurement of the magnetic reconnection rate in the earth's magnetotail. *Journal of Geophysical Research: Space Physics* 123(11): 9150-9168.
- Ni, L., Ji, H., Murphy, N. A. & Jara-Almonte, J. 2020. Magnetic reconnection in partially ionized plasmas. *Proceedings of the Royal Society A.* 476(2236): 20190867.
- Pontin, D. I., Wyper, P. F. & Priest, E. R. 2024. Magnetic reconnection. Dlm. *Magnetohydrodynamic Processes in Solar Plasmas*, 345-414. Elsevier
- Pucci, F., Velli, M., Shi, C., Singh, K., Tenerani, A., Alladio, F., Ambrosino, F., Buratti, P., Fox, W. & Jara-Almonte, J. 2020. Onset of fast magnetic reconnection and particle energization in laboratory and space plasmas. *Journal of Plasma Physics* 86(6): 535860601.

- Rème, H., Aoustin, C., Bosqued, J. M., Dandouras, I., Lavraud, B., Sauvaud, J. A., Barthe, A., Bouyssou, J., Camus, T., Coeur-Joly, O., Cros, A., Cuvilo, J., Ducay, F., Garbarowitz, Y., Medale, J. L., Penou, E., Perrier, H., Romefort, D., Rouzaud, J., Vallat, C., Alcaydé, D., Jacquy, C., Mazelle, C., D'uston, C., Möbius, E., Kistler, L. M., Crocker, K., Granoff, M., Mouikis, C., Popecki, M., Vosbury, M., Klecker, B., Hovestadt, D., Kucharek, H., Kuenneth, E., Paschmann, G., Scholer, M., Sckopke, N., Seidenschwang, E., Carlson, C. W., Curtis, D. W., Ingraham, C., Lin, R. P., Mcfadden, J. P., Parks, G. K., Phan, T., Formisano, V., Amata, E., Bavassano-Cattaneo, M. B., Baldetti, P., Bruno, R., Chionchio, G., Di Lellis, A., Marcucci, M. F., Pallocchia, G., Korth, A., Daly, P. W., Graeve, B., Rosenbauer, H., Vasyliunas, V., Mccarthy, M., Wilber, M., Eliasson, L., Lundin, R., Olsen, S., Shelley, E. G., Fuselier, S., Ghielmetti, A. G., Lennartsson, W., Escoubet, C. P., Balsiger, H., Friedel, R., Cao, J. B., Kovrazhkin, R. A., Papamastorakis, I., Pellat, R., Scudder, J. & Sonnerup, B. 2001. First multispacecraft ion measurements in and near the earth's magnetosphere with the identical Cluster Ion Spectrometry (CIS) experiment. *Ann. Geophys.* 19(10/12): 1303-1354.
- Retinò, A., Nakamura, R., Vaivads, A., Khotyaintsev, Y., Hayakawa, T., Tanaka, K., Kasahara, S., Fujimoto, M., Shinohara, I., Eastwood, J. P., André, M., Baumjohann, W., Daly, P. W., Kronberg, E. A. & Cornilleau-Wehrlin, N. 2008. Cluster observations of energetic electrons and electromagnetic fields within a reconnecting thin current sheet in the earth's magnetotail. *Journal of Geophysical Research: Space Physics* 113(A12)
- Teh, W.-L., Nakamura, R., Fujimoto, M., Kronberg, E. A., Fazakerley, A. N., Daly, P. W. & Baumjohann, W. 2012. Electron dynamics in the reconnection ion diffusion region. *Journal of Geophysical Research: Space Physics* 117(A12)
- Wang, H.-W., Tang, B.-B., Li, W. Y., Zhang, Y.-C., Graham, D. B., Khotyaintsev, Y. V., Gao, C.-H., Guo, X.-C. & Wang, C. 2023. Electron dynamics in the electron current sheet during strong guide-field reconnection. *Geophysical Research Letters* 50(10): e2023GL103046.
- Wilken, B., Daly, P. W., Mall, U., Aarsnes, K., Baker, D. N., Belian, R. D., Blake, J. B., Borg, H., Büchner, J., Carter, M., Fennell, J. F., Friedel, R., Fritz, T. A., Gliem, F., Grande, M., Keckskemety, K., Kettmann, G., Korth, A., Livi, S., Mckenna-Lawlor, S., Mursula, K., Nikutowski, B., Perry, C. H., Pu, Z. Y., Roeder, J., Reeves, G. D., Sarris, E. T., Sandahl, I., Søråas, F., Woch, J. & Zong, Q. G. 2001. First results from the rapid imaging energetic particle spectrometer on board cluster. *Ann. Geophys.* 19(10/12): 1355-1366.